Clinical Cancer Research

B7-H3 Expression in NSCLC and Its Association with B7-H4, PD-L1 and Tumor-Infiltrating Lymphocytes

Mehmet Altan[1,2], Vasiliki Pelekanou[3], Kurt A. Schalper[1,3], Maria Toki[3], Patricia Gaule[3], Konstantinos Syrigos[4], Roy S. Herbst[1], and David L. Rimm[1,3]

Abstract

Purpose: The immune checkpoint PD-1 and its receptor B7-H1 (PD-L1) are successful therapeutic targets in cancer but less is known about other B7 family members. Here, we determined the expression level of B7-H3 protein in non–small cell lung cancer (NSCLC) and evaluated its association with tumor-infiltrating lymphocytes (TIL), PD-L1, B7-H4, and major clinicopathologic characteristics is in 3 NSCLC cohorts.

Experimental design: We used multiplexed automated quantitative immunofluorescence (QIF) to assess the levels of B7-H3, PD-L1, B7-H4, and TILs in 634 NSCLC cases with validated antibodies. Associations between the marker levels, major clinicopathologic variables and survival were analyzed.

Results: Expression of B7-H3 protein was found in 80.4% (510/634) of the cases. High B7-H3 protein level (top 10 percentile) was associated with poor overall survival ($P < 0.05$). Elevated B7-H3 was consistently associated with smoking history across the 3 cohorts, but not with sex, age, clinical stage, and histology. Coexpression of B7-H3 and PD-L1 was found in 17.6% of the cases (112/634) and with B7-H4 in 10% (63/634). B7-H4 and PD-L1 were simultaneously detected only in 1.8% of NSCLCs (12/634). The expression of B7-H3 was not associated with the levels of CD3-, CD8-, and CD20-positive TILs.

Conclusions: B7-H3 protein is expressed in the majority of NSCLCs and is associated with smoking history. High levels of B7-H3 protein have a negative prognostic impact in lung carcinomas. Coexpression of B7-H3 with PD-L1 and B7-H4 is relatively low, suggesting a nonredundant biological role of these targets. *Clin Cancer Res; 23(17); 5202–9. ©2017 AACR.*

Introduction

Immune checkpoints are the T-cell regulatory mechanisms of costimulatory and inhibitory signals that control the amplitude and quality of immune response. The expression of inhibitory immune checkpoints can be upregulated by tumors and serve as an adaptive immune evasion mechanism (1). Activation of the programmed death 1 (PD-1) receptor by its ligand programmed death ligand 1 (PD-L1) has been recognized as a major immunoinhibitory mechanism in solid tumors (2, 3). Although antibodies that inhibit the PD-1/PD-L1 pathway produce durable clinical responses in various solid tumors, including non–small cell lung cancer (NSCLC; refs. 4–7), they only benefit a fraction of patients. Efforts are now focusing on combination strategies to block additional immunosuppressive signals and activate costimulatory receptors to increase response rates, prolong responses, and prevent acquired resistance to monotherapy regimens.

B7-H3 (CD276) is a type I transmembrane protein that belongs to the Ig superfamily and a member of the B7 immunoregulatory molecules (8). Although B7-H3 mRNA is broadly expressed in several organs, including human breast, bladder, liver, lung, lymphoid organs, placenta, prostate and testis (9–11), at the protein level, B7-H3 expression is low and rare (12). B7-H3 upregulation has been reported in multiple malignancies, including NSCLC (13). In preclinical models both stimulatory and inhibitory properties of B7-H3 have been postulated in T-cell–directed cancer immunity (8, 9, 11, 12, 14). In human hepatocellular carcinoma, B7-H3 expression is linked to decreased T-cell proliferation and decreased IFNγ production (15). In murine pancreatic cancer model B7-H3 blockade resulted in an increased $CD8^+$ T-cell influx and antitumor effect (16). In NSCLC, B7-H3 protein expression has been associated with a negative impact in prognosis (17, 18). A humanized, Fc-optimized mAb that targets B7-H3, enoblituzumab (also referred to as MGA271) was shown to produce antitumor responses in a fraction of heavily pretreated solid tumors and was well tolerated at dose levels in a phase I study (19). Currently, clinical activity of enoblituzumab is under investigation as a monotherapy and in combination with either CTLA-4– or PD-L1–targeting mAbs (19, 20). The biologic significance of coexpression of B7 immunoregulatory molecules, their interaction in the tumor microenvironment, and their role in primary and acquired resistance to PD-1 axis inhibitors are unclear.

In this study, we measured the levels of B7-H3 protein both in the tumor and peritumoral stromal tissue, and correlated it with

[1]Section of Medical Oncology, Yale School of Medicine, New Haven, Connecticut. [2]Thoracic/Head and Neck Medical Oncology, MD Anderson Cancer Center, Houston, Texas. [3]Department of Pathology, Yale School of Medicine, New Haven, Connecticut. [4]Third Department of Medicine, University of Athens, School of Medicine, Sotiria General Hospital, Athens, Greece.

Note: Supplementary data for this article are available at Clinical Cancer Research Online (http://clincancerres.aacrjournals.org/).

Corresponding Author: David L. Rimm, Yale University School of Medicine, 310 Cedar Street P.O. Box 208023, New Haven, CT 06520-8023. Phone: 203-737-4204; Fax: 203-737-5089; E-mail: david.rimm@yale.edu

doi: 10.1158/1078-0432.CCR-16-3107

Translational Relevance

The biologic significance of coexpression of B7 immunoregulatory molecules, their interaction and role in primary and acquired resistance to PD-1 axis inhibitors remains unclear. By quantitatively measuring B7-H3, PD-L1 (B7-H1), B7-H4, and tumor-infiltrating lymphocyte subsets in 3 large NSCLC cohorts, we showed that B7-H3 protein is expressed in the majority of NSCLCs, is associated with smoking history and when expressed in high levels is associated with a negative impact on overall survival. We also showed that coexpression of B7-H3 with PD-L1 and B7-H4 is relatively low, and in most of the cases, high protein expression of both proteins does not show colocalization in tumor samples. This somewhat mutually exclusive pattern suggests a nonredundant biological role of these targets, which could support the use of biopsy-driven personalized immunotherapy.

clinicopathological characteristics and outcome in three independent lung cancer cohorts. We have also studied its association with major tumor infiltrating lymphocyte (TIL) subsets, levels of PD-L1, B7-H4 using quantitative objective methods and validated antibodies.

Materials and Methods

Patients, cohorts, and tissue microarrays

Samples from 3 retrospective collections of lung cancer, two from Yale University (Cohort A and Cohort C) and one from University of Athens, Greece (Cohort B) represented in tissue microarrays (TMA) were used. 2 of these cohorts were previously described and include total of 552 formalin-fixed, paraffin-embedded, primary NSCLC tumors samples (Cohort A: 202 and Cohort B: 350 lung carcinomas; refs. 21, 22). A serial collected cohort of patients seen in the Yale Surgical Pathology suite, called YTMA 250, comprises a sample collection from 314 NSCLC patients that had surgical resection of their primary tumor between 2004 and 2011 also used in this study (Cohort C). Clinicopathologic information is summarized in Supplementary Table S1.

For the analysis of B7-H3 tumor and stroma protein expression and their correlation with overall survival, we used 2 different built TMA for the analysis using 0.6 mm tissue cores. These blocks were constructed with the same TMA map but cores obtained by nonadjacent sampling of the same tumors. To address run-to-run variability, slides were stained and analyzed on same days using the same protocol. Serial cut index slides were used for quality control and regression coefficients (R^2) between independent runs for these index slides were found to be high (>0.9). Two TMA histospots were evaluated for each case and average is obtained. Cases that have less than 2% tumor tissue in a histospot have been excluded from the analysis in these cohorts. For the B7-H3 protein expression correlation with PD-L1, B7-H4 protein and TIL subsets; only cases that had staining for all markers included in the correlation studies. All small-cell lung cancer and cell controls within the TMAs excluded for the analysis.

The actual number of samples analyzed for each study is lower due to unavoidable loss of tissue, absence of tumor cells or poor quality of the staining in some spots as is commonly seen in TMA studies. Because of these selection criteria, 130 cases out of 202 cases in Cohort A, 345 cases out of 350 cases in Cohort B and 279 cases out of 314 cases for Cohort C included in the final analysis. All tissue was collected in accordance with US Common Rule after approval from the Yale Human Investigation Committee (also known as the institutional review board) protocol #9505008219, which approved the patient consent forms or in some cases waiver of consent.

Antibody validation

Open-access databases (Expression Atlas European bioinformatics institute EMBL-EBI, https://www.ebi.ac.uk/gxa/home and Cell Line Atlas cell line atlas—The Human Protein Atlas, www.proteinatlas.org/cell) were reviewed for cell line mRNA and protein expression of B7-H3 (CD276). SKBR3 breast cancer cell line was selected because of low mRNA expression. They were obtained from the ATCC and maintained as recommended.

SKBR3 cells were seeded in 24-well plates in duplicates in Gibco RPMI Medium (ThermoFisher Scientific), supplemented with 10% FBS, penicillin–streptomycin (10,000 U/mL) and kept at 37°C, 5% CO_2. When they reached 70% confluency, they were transferred to Optimem-Low Serum Medium (Thermo Fisher Scientific), transfected with 500 ng of B7-H3 plasmid (Provided by Cell Signaling Technology) with different Lipofectamine 2000 Thermo Fisher Scientific, concentrations (2, 3, 4, 5 μL), following the manufacturer's instructions. Empty vector and untreated cells (no plasmid, no Lipofectamine) were also included as negative controls. After 72 hours incubation, cells were collected and replated in 8-chamber polystyrene vessel tissue culture–treated glass slides (Falcon, catalog. no. 354108) in duplicates. Glass slides were washed twice in PBS (Life Technologies) and fixed in 4% Paraformaldehyde for 10 minutes. Then, following double wash in PBS they were permeabilized in 0.2% Triton ×100-PBS for 3 minutes. After a double wash in PBS, a blocking in 2% BSA-PBS for 1 hour at room temperature primary antibodies against cytokeratin (Monoclonal mouse antihuman cytokeratin clone AE1/AE3) and B7-H3 (monoclonal rabbit antibody Cell Signaling Technology, clone D9M2L) were added and left incubate overnight at 4°C, in light protected chamber. Then, after 2 washes of 1% tween-PBS and one in PBS 5 minutes each, secondary antibodies were added using GAM/Alexa Fluor 546 and Rabbit Envision Neat for 1 hour at room temperature. After PBS-tween/PBS wash, Cy5-tyramide (10 μL Cy5 tyramide in 490 Amplification buffer) was added for 10 minutes. Finally, after a last PBS-tween /PBS wash mounting was performed with Prolong Gold—DAPI (Life Technologies).

MCF-7 cell lines were selected for B7-H4 antibody validation using the same cell transfection model described above. Quantitative immunofluorescence (QIF) microscopy used for assessment of protein expression of both positive and negative controls in MCF7 for B7-H4 and SKBR-3 for B7-H3 transfection (Supplementary Figs. S1 and S2).

Quantitative immunofluorescence

B7-H3 (CST; clone D9M2L), PD-L1 (Spring Bioscience; clone SP142), and B7-H4 (CST; clone D1M8I) antibodies were used for staining by using a previously described protocol with simultaneous detection of cytokeratin and DAPI for tumor and nuclear compartment detection, respectively (22). Briefly, TMA slides were baked overnight at 60°C and then soaked in xylene twice for 20 minutes each. Slides were rehydrated in two 1-minute

washes in 100% ethanol followed by one wash in 70% ethanol and finally rinsed in streaming tap water for 5 minutes. Antigen retrieval was performed in the PT module from LabVision for 20 minutes at 97°C in a pressure-boiling container (in sodium citrate buffer, pH 6 for B7-H3 and B7-H4 antibody and with EDTA buffer, pH8 for PD-L1 antibody). Blocking was performed with 0.3% BSA in 0.05% tween solution for 30 minutes after antigen retrieval. Each of the B7 family antibodies (B7H3, B7H4, and PD-L1) was combined with 1:100 pan-cytokeratin antibody (clone AE1/AE3, M3515; Dako Corp.) in 0.3% BSA in TBST and incubated overnight at 4°C. The working concentrations for B7-H3 (clone D9M2L), PD-L1 (SP142) and B7-H4 (D1M8I were 0.05, 0.154, and 1.305 μL/mL, respectively. Primary antibodies were followed by incubation with Alexa 546–conjugated goat anti-mouse or anti-rabbit secondary antibody (Molecular Probes) diluted 1:100 in rabbit or mouse EnVision reagent (Dako) for 1 hour. Signal was amplified with Cyanine 5 (Cy5) directly conjugated to tyramide (PerkinElmer) at 1:50 dilution was used for target antibody detection. ProLong mounting medium (ProLong Gold; Molecular Probes) with 4,6-diamidino-2-phenylindole (DAPI) was used to stain nuclei.

For B7-H3 and B7-H4 colocalization experiments we used a multiplexing protocol that uses benzoic hydrazide with hydrogen peroxide to quench horseradish peroxidase (HRP) activation, as described previously (23). Briefly, following deparaffinization and antigen retrieval (pH 6, Citrate), slides were blocked with 0.3% BSA in Tris-buffered saline/Tween (TBS-T). Primary mAb against B7-H3 (CST, rabbit monoclonal, clone D9M2L), combined with anti-pancytokeratin conjugated with Alexafluor 488 (1:100, eBioscience, clone AE1/AE3 were incubated overnight at 4C. Then, slides were incubated with anti-rabbit Envision reagent (Dako), followed by Cy3 plus tyramide (PerkinElmer; 1:100) amplification for 10 minutes. This step was followed by incubation with 1 mmol/L benzoic hydrazide with 0.15% hydrogen peroxide to quench HRP activation, two times 7 minutes each. Then, slides were incubated with B7-H4 antibody (CST, rabbit monoclonal, clone D1M8I) at 4°C for overnight. On day two, slides were incubated with anti-rabbit Envision reagent (Dako) for an hour at room temperature, followed by signal amplification with Cy-5 tyramide (PerkinElmer; 1:50) for 10 minutes. ProLong mounting medium (ProLong Gold; Molecular Probes) with 4,6-diamidino-2-phenylindole (DAPI) was used to stain nuclei. Between every step, slides were washed with TBS/Tween x2, 5 minutes each followed by TBS wash for 5 minutes.

For B7-H3 and PD-L1 colocalization experiment EDTA pH8 used for antigen retrieval; Primary mAbs against B7-H3 (1:200; CST, Rabbit monoclonal, clone D9M2L), Chicken anti-pancytokeratin with secondary antibody with Alexa Flour 488-conjugated goat anti-chicken and previously validated monoclonal mouse PD-L1 (clone 9A11, CST) antibody (24) used with a multiplexing protocol which was previously described (23).

Quantitative TILs measurement with multiplexing CD3, CD8 and CD20 was described in detail in a previous work of our group (21, 23). In summary CD3, CD8, CD20 and cytokeratin were simultaneously stained in one tissue section using a sequential staining protocol, measurement of TIL markers considered the levels detected in the whole tumor sample (e.g., tumor and stroma). The levels of CD3, CD8, and CD20 were classified as high/low using the median score as cutoff point.

The QIF measurements were performed using the AQUA method of QIF (Genoptix Medical Laboratory) as previously described (25). The QIF score of B7-H3 antibody in the tumor and in the stroma was calculated by dividing the target B7-H3 pixel intensity in the area of the tumor and stroma compartment defined by the cytokeratin and DAPI positivity in TMA slides containing the cohort cases. Serial section slides measuring PD-L1 (SP142, Spring), and B7-H4 (D1M8I, Cell Signaling Technology) protein expression were used for the assessment of mutual expression rates between these 3 markers and their association with TILs.

Statistical analysis

Pearson's correlation coefficient (R) was used to assess the reproducibility of the assay between near-serial sections of the index array. Differences between QIF signals between groups were analyzed using the Fisher's exact test two-sided. *P* values were considered statistically significant if <0.05. Linear regression coefficients were calculated to determine the association between continuous scores. For all Cohorts (A, B, C), B7-H3, PD-L1 and B7-H4 AQUA scores from two independent cores for each histospot were averaged and the averages were used for final analysis. A visual cut-off point was determined for each cohort for QIF positivity. Survival functions were compared using Kaplan–Meier curves, and statistical significance was determined using the log-rank test. Survival analysis of continuous marker scores was performed using the X-tile software (Yale University, New Haven, CT) for disease-specific survival differences (26). GraphPad Prism 7.01 software was used to generate Kaplan–Meier survival analysis.

Results

In NSCLC tissues B7-H3 protein expression showed a predominant cytoplasmic and membranous distribution in tumor cells (Fig. 1). Protein expression of B7-H3 was significantly higher in the tumor compartment than in stroma and the correlation was low (linear correlation coefficient [R^2] of 0.25 (Supplementary Fig. S3). Because the levels of stromal B7H3 were generally low, the remainder of this work focuses on the tumor cell expression only. The levels of tumor cell B7-H3 in the lung cohorts showed a continuous distribution. A visual cutoff point was determined for each cohort for QIF positivity and of the 634 cases represented in 3 cohorts B7-H3 protein expression was found in 80.4% (510/634) of cases (99/118 [83%] in cohort A, 255/291 [87%] cohort B; and 156/225 [69%] cohort C (Fig. 1). Per this signal detection threshold, B7-H3 protein expression did not correlate with survival in positive and negative cases. By using X-tile, Cohort A was used as a training set to explore possible prognostic effect of B7-H3 protein expression for different expression levels. In the highest 10%, B7-H3 protein expression was found to be significantly associated with poor overall survival and this cutoff value was validated in two independent cohorts ($P < 0.05$; Fig. 2). Elevated tumor and stromal B7-H3 expression was consistently associated with smoking history across the 3 cohorts, but not with sex, age, clinical stage, and histology (Table 1). In cox regression model the negative impact of high tumor B7-H3 tumor protein expression to overall survival remained significant in 2 cohorts while there was a trend on which was not statistically significant in a third cohort (Supplementary Table S2.)

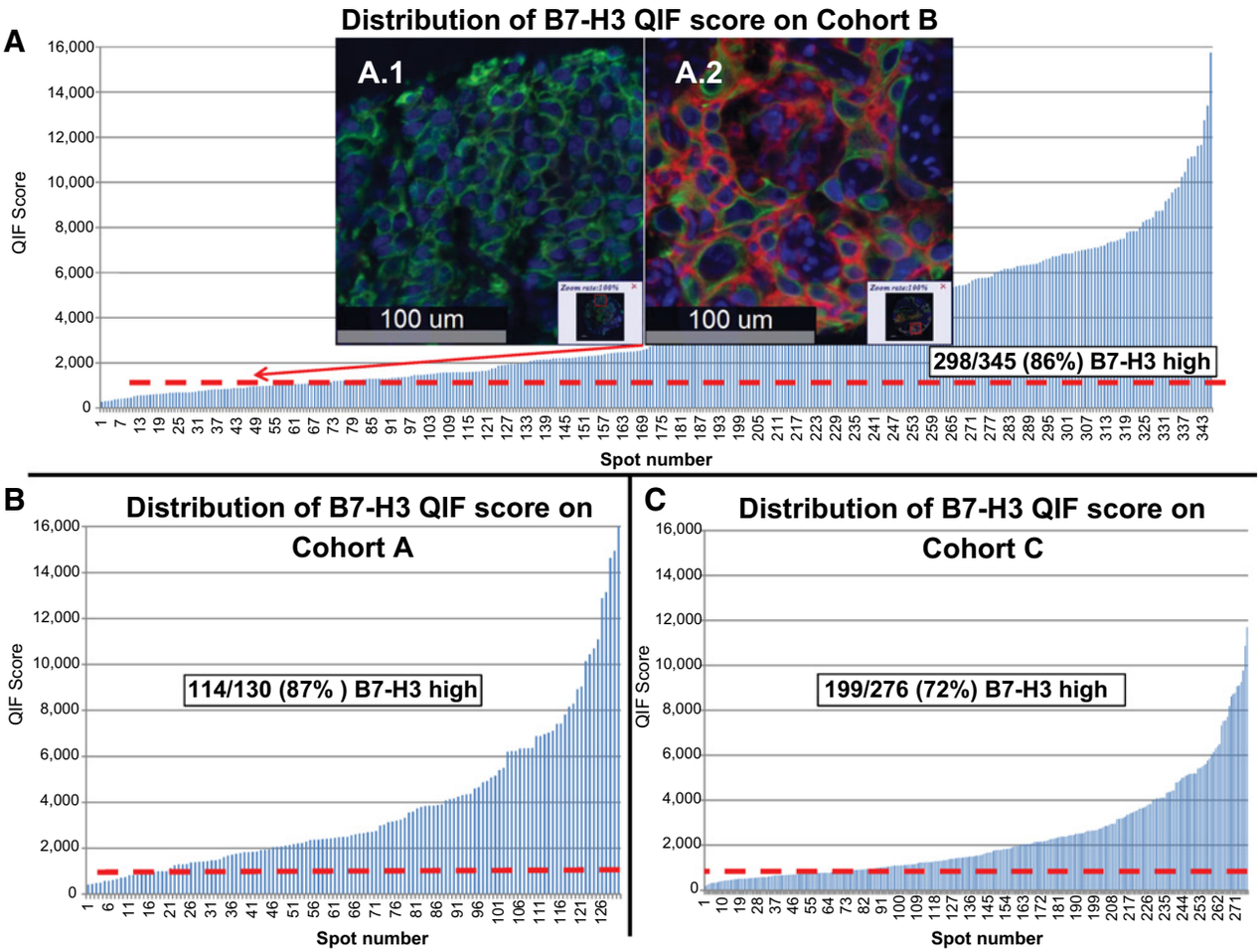

Figure 1.

A, QIF score distribution of tumor B7-H3 protein expression in Cohort B. Scores are expressed as arbitrary units of fluorescence and the dashed red line indicates the signal detection threshold determined by a visual cutoff as described in Materials and Methods; A1 and A2 are examples of TMA spots with negative and positive B7-H3 signal, respectively [DAPI in blue, Cytokeratin mask in green (Cy3 channel) and B7-H3 is in red (Cy5 channel]; **B** and **C,** QIF score distribution of tumor B7-H3 in Cohort A and C, respectively.

In a merged analysis of the three cohorts, B7-H3 and PD-L1 coexpression was observed in 17.6% (112/634) of all cases (Cohort A: 19/118 [16%], Cohort B 71/291 [24%], Cohort C 22/225 [9%]); B7-H3 and B7-H4 coexpression was observed in 10% (63/634) of the cases (Cohort A: 22/118 [18%], Cohort B 19/291 [6%], Cohort C 22/225 [9%]), B7-H4 and PD-L1 coexpression was observed in 1.8% (12/634) of all cases (Cohort A: 5/118 [4%], Cohort B 5/291[2%], Cohort C 2/225 [1%]). Figure 3 shows the somewhat mutually exclusive expression in the combined cohorts. In tumor samples where high protein expression is observed for multiple markers of interest (coexpression), multiplexing experiments were conducted to further assess for colocalization of these markers with-in same cell. In most of the cases with high B7-H3 and B7-H4 protein expression, tumor tissue did not show colocalization of these proteins (Figs. 3 and 4). Tumors showing high levels of PD-L1 and B7-H3 showed focal colocalization (Supplementary Fig. S4 and S5) in most of the samples. B7-H4 and PD-L1 multiplexed colocalization assessment was not studied since these proteins are mutually exclusive in our cohorts.

Neither tumor nor stromal B7-H3 expression showed any correlation with major TIL subtypes.

Discussion

Here, we show that B7-H3 protein is widely expressed in the majority of NSCLCs and is associated with smoking history. In all three cohorts, overexpression of B7-H3 protein (highest 10%) was correlated with poor survival. This association indicates a prognostic effect consistent with previous observations in NSCLC cohorts (17). Coexpression or mutual exclusivity of an immune checkpoint may support understanding the mechanistic differences that affects the tumor microenvironment and tumor immune evasion. In this study, elevated levels of B7-H3 were not associated with lymphocyte infiltration, including CD8 (+) lymphocyte subpopulations, suggesting that B7-H3

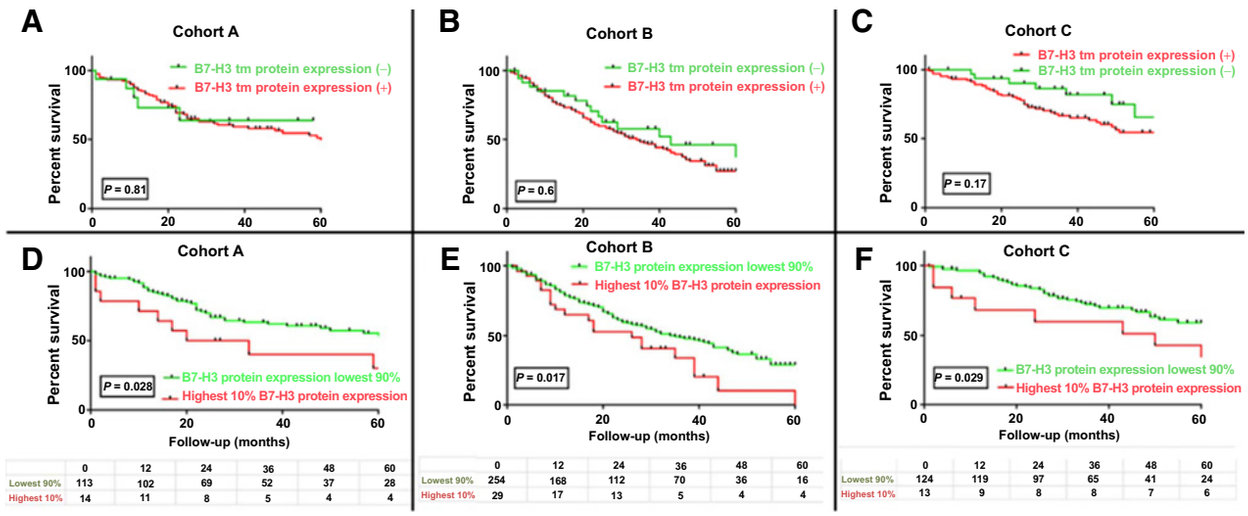

Figure 2.

Kaplan–Meier overall survival curve in 3 cohorts; **A–C,** Tumor (tm) B7-H3 QIF-positive and -negative cases (red, positive; green, negative) in Cohort A, B, and C, respectively. **D–F,** Highest 10% QIF tumor B7-H3 QIF score as a cut-off value in Cohort A, B, and C, respectively (red: B7-H3 protein expression highest 10%, green: B7-H3 protein expression lowest or negative 90%).

expression/upregulation is IFN-γ independent. Furthermore, B7-H3 and PD-L1 protein coexpression was observed in only 18% of the cases, only somewhat mutually exclusive as compared to nearly complete lack of coexpression observed for PD-L1 and B7-H4. This is suggestive of a non-redundant biological role for these targets. B7-H3 and B7-H4 coexpression was relatively low. In most of the cases high protein expression of both proteins did not show colocalization. This exclusive pattern with infrequent coexpression and colocalization is suggesting that some lung tumors may preferentially use one

Table 1. Tumor B7-H3 QIF and its correlation with clinicopathologic features and with lymphocyte subtypes

	Cohort A			Cohort B			Cohort C		
Characteristics	**B7-H3 (-)**	**B7-H3 (+)**	***P***	**B7-H3 (-)**	**B7-H3 (+)**	***P***	**B7-H3 (-)**	**B7-H3 (+)**	***P***
Sex									
Male	8	56	0.31	32	192	0.18	34	70	0.56
Female	11	43		2	36		35	86	
Unknown				2	27				
Age									
<70 y	11	59	1	30	173	0.18	43	88	0.46
≥70 y	8	40		4	53		26	68	
Unknown				2	29				
Stage									
III	14	67	0.78	19	139	1	59	124	0.35
III–IV	5	32		13	90		10	32	
Unknown				4	26				
Histology									
ADC	15	67	0.03	17	96	0.4	51	94	0.33
SCC	0	22		15	117		17	45	
Other	4	10		0	16		1	17	
Unknown				4	26				
Smoker									
Current/former	15	94	0.03	24	192	0.05	47	129	0.02
Non-smoker	4	5		6	17		16	18	
Unknown				6	46		6	9	
CD3									
Low	10	48	0.8	21	124	0.29	32	81	0.47
High	9	51		15	131		37	75	
CD8									
Low	9	51	0.8	17	129	0.72	32	81	0.47
High	10	48		19	126		37	75	
CD20									
Low	8	50	0.61	22	124	0.21	40	73	0.14
High	11	49		14	132		29	83	

Abbreviations: ADC, adenocarcinoma; SCC, squamous cell carcinoma.

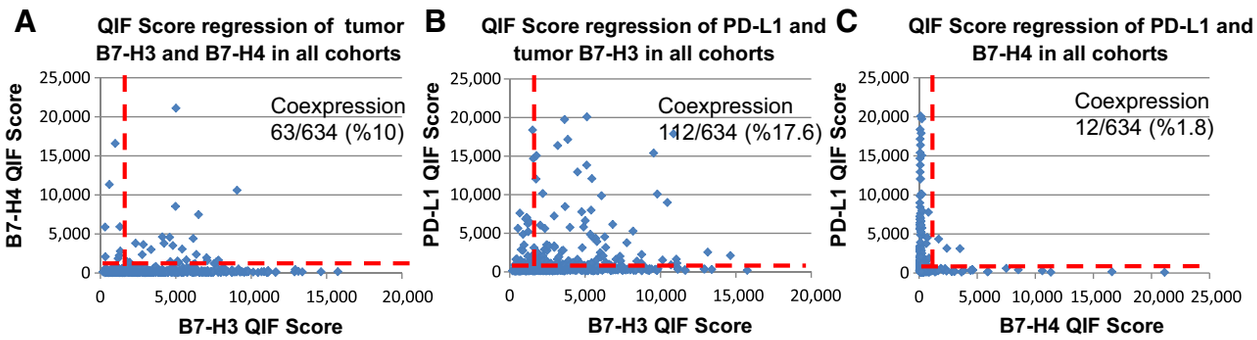

Figure 3.

A–C, QIF score regressions of markers the dashed red line indicates the signal detection threshold determined by visual cutoff. **A,** QIF score regressions for coexpression rates of tumor B7-H3 and B7-H4 protein; **B,** QIF score regressions for coexpression rates of tumor PD-L1 and B7-H3 protein; **C,** QIF score regressions for coexpression rates of tumor PD-L1 and B7-H4 protein.

immune evasion mechanism/pathway. Future studies with longitudinal samples (e.g. repeat biopsy protocols) especially in acquired resistance to immunotherapy to assess the spatio-temporal dynamics of the tumor microenvironment and assessment of coexpression rates of immune checkpoints in biopsy specimens may answer this question.

Although drug development to target B7-H4 is ongoing (27), an anti–B7-H3 mAb, MGA271 (Enoblituzumab; ref. 20), has been shown to be tolerable in a phase I study in solid tumors (19). Currently multiple phase I/II studies are ongoing to assess its safety and efficacy as a single agent and in combination with PD-1/PD-L1 or CTLA-4 axis blockers. With given different coexpression rates of B7 family immune checkpoints in NSCLC, it is useful to explore combination strategies to block additional immunosuppressive signals toward the goals of increasing response rates, prolonging responses, and prevention of acquired resistance to monotherapy regimens.

There are a number of limitations to this study. The cohorts represented on our TMAs were entirely retrospectively collected samples from cases with variable follow-up, different treatments and pre-dating molecular/genomic annotation. Because of these limitations to avoid premature conclusions maybe related selection bias, we highlighted the findings that are consistent in all cohorts. Although the mechanism of B7-H3 protein overexpression in tumors are unclear, in our analysis B7-H3 expression was not correlated to histology, tumor stage or patients age but was correlated to smoking status. The similar B7H3 protein expression in 3 cohorts with different

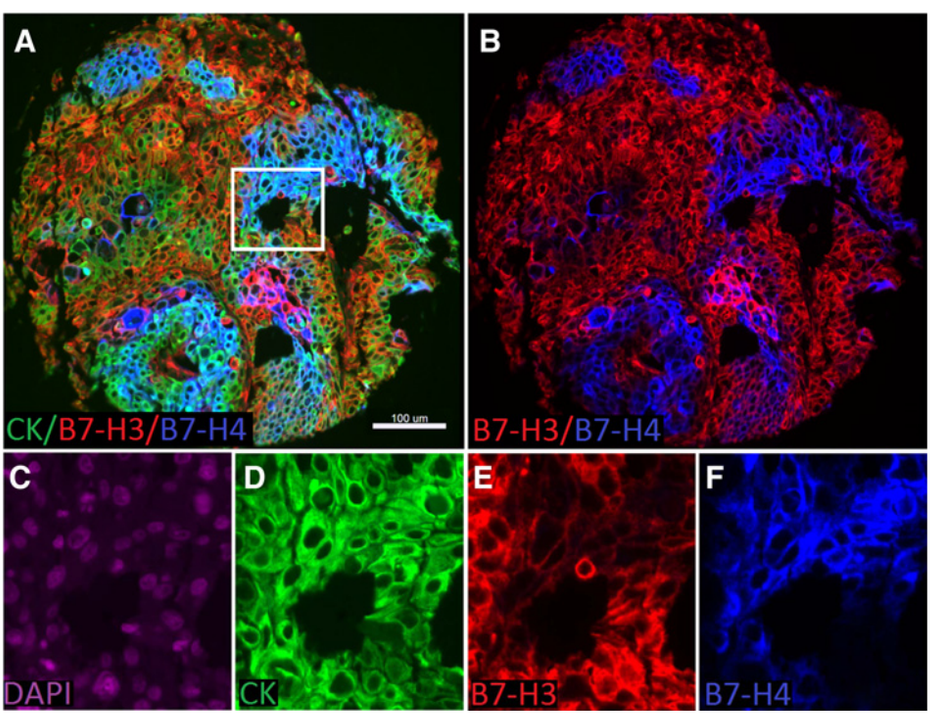

Figure 4.

Detection of B7-H3 and B7-H4 protein expression to assess colocalization using immunofluorescence (QIF) in lung cancer. **A,** Representative fluorescence images showing the simultaneous detection of B7-H3 (red channel), B7-H4 (blue channel), and cytokeratin (green channel, inserted box is highlighting the area that has been magnified in Fig. 2C–F. Simultaneous detection of B7-H3 (red channel), B7-H4 (blue channel; **B**); 4′,6-diamidino-2-phenylindole (DAPI) only in purple channel (**C**); Cytokeratin only in green channel (**D**); B7-H3 only in red channel (**E**); and B7-H4 only in blue channel (**F**); scale bar, 100 µm.

histopathologic distribution may be associated with other factors such as the host immune system. This work was performed on TMAs that may induce under or overrepresentation of the marker levels due to tumor heterogeneity, and therefore may not mirror clinical samples studied using whole-tissue sections. This is a critical point, because we have found prognostic significance in only the highest 10% tumor B7-H3 tumor protein expression. In this study, the proportion of lung cancer cases showing PD-L1 and B7-H4 expression in these cohorts is not identical with our previous reports. This difference is likely due to unavoidable loss of tissue or the absence or limited tumor cells in some spots in different cuts as which is commonly seen in TMA studies.

In summary, we find expression of B7-H3 is more frequent in NSCLC than any previously described immune checkpoint ligand. It's somewhat mutually exclusive expression pattern with respect to other checkpoints is encouraging with respect to potential for complementary therapeutic approaches. We hope this study can lead to further clinical exploration of these checkpoint-targeting agents in clinical trials, which could play a relevant role in lung cancer clinical trial designs for combination immunotherapy strategies.

Disclosure of Potential Conflicts of Interest

K.A. Schalper is a consultant/advisory board member for Viralytics, and reports receiving commercial research grants from Onkaido, Takeda, Tesaro, and Vasculox. D.L. Rimm is a consultant/advisory board member for AstraZeneca, Bristol-Myers Squibb, Cell Signaling Technology, PerkinElmer, and Ultivue. No potential conflicts of interest were disclosed by the other authors.

Authors' Contributions

Conception and design: M. Altan, V. Pelekanou, K.A. Schalper, R.S. Herbst, D.L. Rimm

Development of methodology: M. Altan, V. Pelekanou, R.S. Herbst, D.L. Rimm

Acquisition of data (provided animals, acquired and managed patients, provided facilities, etc.): M. Altan, V. Pelekanou, M. Toki, P. Gaule, K. Syrigos, R.S. Herbst, D.L. Rimm

Analysis and interpretation of data (e.g., statistical analysis, biostatistics, computational analysis): M. Altan, V. Pelekanou, K.A. Schalper, M. Toki, K. Syrigos, R.S. Herbst, D.L. Rimm

Writing, review, and/or revision of the manuscript: M. Altan, V. Pelekanou, K.A. Schalper, P. Gaule, K. Syrigos, R.S. Herbst, D.L. Rimm

Administrative, technical, or material support (i.e., reporting or organizing data, constructing databases): M. Altan, K. Syrigos, R.S. Herbst, D.L. Rimm

Study supervision: D.L. Rimm

Grant Support

This work was supported by grants from the Yale SPORE in Lung Cancer P50CA196530 (principal investigator: R.S. Herbst), and sponsored research agreements from Genoptix (principal investigator: D.L. Rimm) and Gilead Sciences Inc (subcontract principal investigator: D.L. Rimm).

The costs of publication of this article were defrayed in part by the payment of page charges. This article must therefore be hereby marked *advertisement* in accordance with 18 U.S.C. Section 1734 solely to indicate this fact.

Received December 13, 2016; revised February 13, 2017; accepted May 16, 2017; published OnlineFirst May 24, 2017.

References

1. Pardoll DM. The blockade of immune checkpoints in cancer immunotherapy. Nat Rev Cancer 2012;12:252–64.
2. Keir ME, Butte MJ, Freeman GJ, Sharpe AH. PD-1 and its ligands in tolerance and immunity. Annu Rev Immunol 2008;26:677–704.
3. Sharpe AH, Wherry EJ, Ahmed R, Freeman GJ. The function of programmed cell death 1 and its ligands in regulating autoimmunity and infection. Nat Immunol 2007;8:239–45.
4. Brahmer JR, Tykodi SS, Chow LQ, Hwu WJ, Topalian SL, Hwu P, et al. Safety and activity of anti-PD-L1 antibody in patients with advanced cancer. N Engl J Med 2012;366:2455–65.
5. Brahmer JR, Drake CG, Wollner I, Powderly JD, Picus J, Sharfman WH, et al. Phase I study of single-agent anti-programmed death-1 (MDX-1106) in refractory solid tumors: safety, clinical activity, pharmacodynamics, and immunologic correlates. J Clin Oncol 2010;28:3167–75.
6. Topalian SL, Hodi FS, Brahmer JR, Gettinger SN, Smith DC, McDermott DF, et al. Safety, activity, and immune correlates of anti-PD-1 antibody in cancer. N Engl J Med 2012;366:2443–54.
7. Topalian SL, Sznol M, McDermott DF, Kluger HM, Carvajal RD, Sharfman WH, et al. Survival, durable tumor remission, and long-term safety in patients with advanced melanoma receiving nivolumab. J Clin Oncol 2014;32:1020–30.
8. Zou W, Chen L. Inhibitory B7-family molecules in the tumour microenvironment. Nat Rev Immunol. 2008;8:467–77.
9. Hofmeyer KA, Ray A, Zang X. The contrasting role of B7-H3. Proc Nat Acad Sci USA 2008;105:10277–8.
10. Sun M, Richards S, Prasad DV, Mai XM, Rudensky A, Dong C. Characterization of mouse and human B7-H3 genes. J Immunol 2002;168:6294–7.
11. Chapoval AI, Ni J, Lau JS, Wilcox RA, Flies DB, Liu D, et al. B7-H3: a costimulatory molecule for T cell activation and IFN-gamma production. Nat Immunol 2001;2:269–74.
12. Yi KH, Chen L. Fine tuning the immune response through B7-H3 and B7-H4. Immunol Rev 2009;229:145–51.
13. Sun Y, Wang Y, Zhao J, Gu M, Giscombe R, Lefvert AK, et al. B7-H3 and B7-H4 expression in non-small-cell lung cancer. Lung Cancer 2006;53:143–51.
14. Kreymborg K, Haak S, Murali R, Wei J, Waitz R, Gasteiger G, et al. Ablation of B7-H3 but not B7-H4 results in highly increased tumor burden in a murine model of spontaneous prostate cancer. Cancer Immunol Res 2015;3:849–54.
15. Sun TW, Gao Q, Qiu SJ, Zhou J, Wang XY, Yi Y, et al. B7-H3 is expressed in human hepatocellular carcinoma and is associated with tumor aggressiveness and postoperative recurrence. Cancer Immunol Immunother 2012;61:2171–82.
16. Yamato I, Sho M, Nomi T, Akahori T, Shimada K, Hotta K, et al. Clinical importance of B7-H3 expression in human pancreatic cancer. Br J Cancer 2009;101:1709–16.
17. Lou Y, Diao L, Cuentas ER, Denning WL, Chen L, Fan YH, et al. Epithelial-mesenchymal transition is associated with a distinct tumor microenvironment including elevation of inflammatory signals and multiple immune checkpoints in lung adenocarcinoma. Clin Cancer Res 2016;22:3630–42.
18. Danilova L, Wang H, Sunshine J, Kaunitz GJ, Cottrell TR, Xu H, et al. Association of PD-1/PD-L axis expression with cytolytic activity, mutational load, and prognosis in melanoma and other solid tumors. Proc Nat Acad Sci USA 2016;113:E7769–e77.
19. Powerly J, Cote G, Flaherty K, Szmulewitz R, Ribas A, Weber JS, et al. Interim results of an ongoing phase 1, dose escalation study of MGA271 (Enoblituzumab), an Fc-optimized humanized anti-B7-H3 monoclonal antibody, in patients with advanced solid cancer. J Immuno Ther Cancer 2015;3:8.
20. Loo D, Alderson RF, Chen FZ, Huang L, Zhang W, Gorlatov S, et al. Development of an Fc-enhanced anti-B7-H3 monoclonal antibody with potent antitumor activity. Clin Cancer Res 2012;18:3834–45.
21. Schalper KA, Brown J, Carvajal-Hausdorf D, McLaughlin J, Velcheti V, Syrigos KN, et al. Objective measurement and clinical significance of TILs in non–small cell lung cancer. J Natl Cancer Inst 2015;107. pii: dju435.

22. Velcheti V, Schalper KA, Carvajal DE, Anagnostou VK, Syrigos KN, Sznol M, et al. Programmed death ligand-1 expression in non–small cell lung cancer. Lab Invest 2014;94:107–16.
23. Brown JR, Wimberly H, Lannin DR, Nixon C, Rimm DL, Bossuyt V. Multiplexed quantitative analysis of CD3, CD8, and CD20 predicts response to neoadjuvant chemotherapy in breast cancer. Clin Cancer Res 2014;20:5995–6005.
24. Gaule P, Smithy JW, Toki M, Rehman J, Patell-Socha F, Cougot D, et al. A quantitative comparison of antibodies to programmed cell death 1 Ligand 1. JAMA Oncol 2016 Aug 18. [Epub ahead of print].
25. Camp RL, Chung GG, Rimm DL. Automated subcellular localization and quantification of protein expression in tissue microarrays. Nat Med. 2002;8:1323–7.
26. Camp RL, Dolled-Filhart M, Rimm DL. X-tile: a new bio-informatics tool for biomarker assessment and outcome-based cut-point optimization. Clin Cancer Res 2004;10: 7252–9.
27. Leong SR, Liang WC, Wu Y, Crocker L, Cheng E, Sampath D, et al. An anti-B7-H4 antibody-drug conjugate for the treatment of breast cancer. Mol Pharm 2015;12:1717–29.